Neoplasma 2026; 73(2): 133–145

doi:10.4149/neo_2026_251124N495

circRNA circ-ZEB1 promotes gallbladder carcinomas progression by regulating the miR-144-3p/ZEB2 axis

Luoshun HUANG#, Yang ZHANG#, Fan YANG, Yisheng LING, Xianfei ZHOU*

Department of Hepatobiliary Surgery, Taizhou Municipal Hospital (Taizhou University Affiliated Municipal Hospital), School of Medicine, Taizhou University, Taizhou, Zhejiang, China

**Correspondence: slyy_01740@tzc.edu.cn*
#Contributed equally to this work.

Received November 24, 2025 / Accepted March 27, 2026

Gallbladder cancer (GBC) is the most common and aggressive type of tumor occurring in the biliary system. Several studies have indicated the possible functions of circular RNAs (circRNAs) in GBC tumorigenesis. This research aimed to explore the roles of a novel circRNA, circ-ZEB1 (hsa_circ_0093509), in GBC. The expressions of circ-ZEB1, miR-144-3p, and ZEB2 in GBC cells were detected using RT-qPCR or western blot. The subcellular localization of circ-ZEB1 in GBC cells was determined. The function of circ-ZEB1, miR-144-3p, and ZEB2 in GBC cells was assessed by using CCK-8, EdU staining, colony formation, or Transwell assays. The relationship among miR-144-3p and corresponding targets, circ-ZEB1 and ZEB2, was confirmed. Additionally, xenograft experiments were conducted to assess the role of circ-ZEB1 in tumor growth in vivo. circ-ZEB1 was predominantly found in the cytoplasmic region of GBC cells and was upregulated in the GBC cell lines. Suppression of circ-ZEB1 reduced the proliferation and migration of GBC-SD and SGC-996 cells. Knockdown of circ-ZEB1 attenuates tumor growth in vivo. Mechanistically, circ-ZEB1 sponged miR-144-3p, which targeted ZEB2. Additionally, inhibition of miR-144-3p rescues the effects of circ-ZEB1 or ZEB2 knockdown. These results clarified a vital role of the circ-ZEB1/miR-144-3p/ZEB2 axis in GBC advancement, and may serve as a novel therapeutic target for GBC treatment.

Key words: gallbladder carcinoma; circRNA; miR-144; ZEB2; migration

Gallbladder carcinoma (GBC) is one of the deadliest cancers of the digestive tract [1, 2]. Characterized by insidious onset, rapid progression, early metastasis, and profound therapy resistance, GBC portends a dismal prognosis [3, 4]. Key risk factors include chronic inflammation, gallstones, gallbladder polyps (> 1 cm), obesity, and diabetes, with gallstone-associated cholecystitis being the most prevalent precursor [5]. Despite surgical resection remaining the primary curative modality, supplemented by adjuvant radiotherapy and chemotherapy, survival benefits remain marginal [6, 7]. The emergence of targeted therapies and immunotherapy has yielded limited success in GBC. There is a serious need to identify novel therapeutic targets.

Circular RNAs (circRNAs) are a large class of non-coding RNAs generated by back-splicing events [8, 9]. Because they lack free 5' caps and 3' poly-(A) tails, circRNAs are highly resistant to exonucleases and exhibit half-lives that greatly exceed those of linear transcripts [10]. Mounting evidence indicates that circRNAs are not merely splicing noise but rather potent regulators of gene expression that function as microRNA (miRNA) sponges, scaffolds for RNA-binding proteins, transcriptional modulators, and even templates for translation [11, 12]. In biliary tract cancers, dysregulated circRNAs – such as circRNA_CDKN1A, circSMAD2, and circPCNXL2-have been shown to promote proliferation, epithelial-mesenchymal transition (EMT), and chemoresistance by sequestering tumor-suppressive miRNAs or by stabilizing oncogenic messenger RNAs [13–15]. Despite these insights, the global landscape of circRNA dysregulation in GBC remains fragmentary, and only a handful of circRNAs have been functionally validated.

circ-ZEB1 (hsa_circ_0093509) is increasingly recognized as a potent oncogene derived from exons 4–8 of the ZEB1 (NM_001128128) on chromosome 10 (31749965–31803636). ZEB1 is a master transcriptional repressor of E-cadherin and a key driver of EMT in multiple solid tumors [16, 17]. While

the linear ZEB1 transcript has been extensively studied, the biological roles of its circular counterpart have only recently begun to emerge. In liver cancer, Liu et al. reported that circ-ZEB1 is markedly upregulated and increases PIK3CA by sponging miR-199a-3p, thereby enhancing proliferation and inhibiting apoptosis [18]. Chen and colleagues subsequently demonstrated that circ-ZEB1 exhibits elevated expression levels in colorectal cancer tissues, where it sequesters miR-200c-5p to foster EMT and oxaliplatin resistance [19]. More recently, Wang et al. showed that circ-ZEB1 is elevated in lung cancer and accelerates metastasis via the miR-491-5p/EIF5A axis [20]. Collectively, these findings establish circ-ZEB1 as a conserved oncogenic circRNA across diverse epithelial malignancies. However, to date, no reports have documented dysregulation of circ-ZEB1 in GBC.

In this study, we aimed to illuminate a previously unrecognized circRNA-mediated circuitry in GBC and to identify the translational potential of targeting circ-ZEB1. *In vitro* and *in vivo* functional experiments demonstrated that the knockdown of circ-ZEB1 inhibited the proliferation and metastasis of GBC cells. Mechanistically, circ-ZEB1 functions as a miR-144-3p sponge to regulate GBC progression via the miR-144-3p/ZEB2 axis. These findings establish circ-ZEB1 as a potential tumor biomarker and promising therapeutic target, providing new insights into GBC pathogenesis and offering a foundation for novel diagnostic and therapeutic strategies.

Materials and methods

Cell culture. Normal human gallbladder epithelial cells (HGBEC) and GBC cell lines (NOZ, GBC-SD, G-415, and SGC-996) were acquired from the American Type Culture Collection (ATCC, USA). Human GBC cell line OCUG-1 was obtained from the Jennio Biotech Co., Ltd. (Guangzhou, China). The HGBEC were cultured in DMEM (GNM12800, GENOM Biotech, Zhejiang, China) with 10% FBS (#BS1105, Opcel, Nei Monggol, China), and the GBC cells were maintained in RPMI-1640 (#GNM31800, GENOM Biotech) supplemented with 10% FBS. The cells were maintained in a 37 °C incubator with 5% CO_2 and a humidified environment. The medium was replaced every three days.

Actinomycin D and RNase R treatment. Total RNA of GBC-SD cells was isolated utilizing TRIzol reagent (#15596-026, Invitrogen, USA). For the actinomycin D test, GBC-SD cells were treated with actinomycin D (5 μg/ml, #HY-17559, MCE, USA). Next, the cells were collected at the specified time intervals (0 h, 4 h, 8 h, 12 h, and 24 h), respectively. For the RNase R treatment, 5 μg of total RNA from GBC-SD cells was incubated with 3 U/μg RNase R (#19101, Qiagen, USA), followed by assessing the stabilities of circ-ZEB1 and linear ZEB1 mRNA utilizing RT-qPCR analysis.

Fluorescence *in situ* hybridization analysis (FISH) assay. FISH assays were conducted using a FISH kit from Genepharma (Shanghai, China). The circ-ZEB1 was designed by GenePharma (Shanghai, China), and its probe was labeled with Cy3. Following the protocol provided by the FISH kit, fluorescence images were captured using a microscope (LSM880, Carl Zeiss, Germany).

Nuclear and cytoplasmic extraction. RNA of nuclear and cytoplasmic fractions from GBC-SD and SGC-996 cells was obtained using NE-PER Kit (#78835, Thermo Fisher Scientific, USA) in accordance with the manufacturer's guidelines. Next, the expression of U6, GAPDH, and circ-ZEB1 was detected by RT-qPCR.

Cell transfection. Short hairpin oligonucleotides (shRNAs) and normal control (sh-NC) targeting circ-ZEB1 (shRNA-#1, shRNA-#2, and shRNA-#3) were provided by GenePharma. miR-144-3p mimics/inhibitors and their NC were produced by RiboBio (Guangzhou, China). All sequences were listed in Supplementary Table S1. Cell transfection was conducted in GBC-SD and SGC-996 cells utilizing Lipofectamine 3000 (#L3000-008, Invitrogen, USA). Following a 48 h period post-transfection, the efficiency of transfection was explored by using RT-qPCR assays.

CCK-8 and EdU assay. GBC cells that had undergone transfection were placed into a 96-well plate. At 24, 48, or 72 h following inoculation, CCK-8 (10 μl, #C0039, Beyotime, China) was added into the wells, followed by an incubation for 2 h at 37 °C. Then, absorbance at 450 nm was measured to determine cell viability using a microplate reader (CMaxPlus, Molecular Devices). For the EdU assay, BeyoClick™ EdU Cell Proliferation Kit with AF594 (#C0078S, Beyotime) was used to estimate the proliferation ability of transfected GBC-SD and SGC-996 cells. Transfected cells were plated in 12-well plates and incubated for 24 h. Then, EdU solution (50 μM) in 500 μl was added to the cells and incubated for 2 h. Subsequently, the cells were fixed, permeabilized, and incubated with the click additive solution for 30 min. At last, the DAPI solution was used and incubated for 5 min to stain the nuclei. Images of EdU-positive cells were captured under an inverted fluorescence microscope (Ts2-FC, Nikon, Japan) and counted using ImageJ software.

Colony formation assay. Transfected GBC cells were placed into 24-well plates at a density of 500 cells/well and cultured for 14 days. Following fixation, the cells were treated with 0.1% crystal violet (#Y268091, Beyotime, China) for 15 min. The colonies were subsequently enumerated using a light microscope (ICX41, Sunny Optical Technology (group) Co., Ltd., Zhejiang, China).

Transwell assay. Transwell inserts (CLS3428-24EA, Corning, USA) with 8-μm pore membranes were used to evaluate cell migration and invasion. For the migration assay, 600 μl of medium augmented with 10% FBS was placed in the lower chamber. Transfected GBC-SD and SGC-996 cells were seeded in the upper chamber with 200 μl of medium that contained 1% FBS and incubated for 24 h at 37 °C. Cells that migrated to the lower membrane surface were fixed and stained with 0.1% crystal violet for 30 min. Representative images were obtained under a microscope,

and the number of migrating cells was counted from three randomly chosen fields. For the invasion assay, the inserts were treated with a Matrigel matrix (#356234, BD Science, USA). The subsequent steps were analogous to those of the migration assay.

Luciferase reporter assay. The wild type (WT) and mutant (MUT) miR-144-3p binding site sequences of circ-ZEB1 and ZEB2 were respectively inserted into p-mirGLO basic reporter vectors (#E2940, Promega, USA) to create the respective vectors (circ-ZEB1-WT/MUT and ZEB2 3'UTR-WT/MUT). Subsequently, GBC cells were introduced to the reporter vectors along with either a miR-144-3p mimic or a miR-NC. The luciferase activities were observed using the Dual Luciferase Reporter Gene Assay Kit (#RG027, Beyotime, Shanghai, China).

RNA-protein immunoprecipitation (RIP) assay. RIP assays were carried out utilizing a Magna RIP RNA Immunoprecipitation Kit (Millipore-MAGNARIP02, Millipore, USA). Cell extracts from GBC-SD and SGC-996 cells were administered with protein A magnetic beads conjugated to either anti-Ago2 or IgG antibody. After RNA complexes were purified, the levels of circ-ZEB1 and miR-144-3p were assessed using RT-qPCR assays.

Xenograft mouse model. Five-week-old male BALB/c nude mice (SLAC Laboratory Animal Co., Ltd., Shanghai, China) were randomly divided into 2 groups, with 6 in each group. Following transfection with either sh-circ-ZEB1#1 or sh-NC, GBC-SD cells were resuspended in PBS (2×10^6 cells/200 μl) for subcutaneous injection into the right flank of nude mice. After that, the tumor size was recorded every 7 days and calculated as $V = (\text{length} \times \text{width}^2)/2$. On the 28th day, the mice were sacrificed by cervical dislocation after being anesthetized using 1% pentobarbitalum natricum (50 mg/kg, i.p, Sigma-Aldrich), and then the tumor samples were gathered and weighed. Finally, the tumor samples were stored at –80 °C and used for immunohistochemical (IHC) experiments. This study was approved by the Ethics Committee of Hunter BioInsight Technology, Inc (Approval No. IACUC/HTYJ-8201-126, Zhejiang, China) and conducted in compliance with the National Institutes of Health Guide for the Care and Use of Laboratory Animals (NIH Publications No. 8023, revised 1978).

IHC assay. All tumor samples were fixed with 4% paraformaldehyde for 24 h before serial sectioning at 2 μm using a microtome (RM2016, Leica, Germany). The paraffin sections were soaked in xylene and graded ethanol for deparaffinization and hydration. Following antigen restoration, the activity of endogenous peroxidase was inhibited and subsequently blocked using 5% BSA, the sections were treated with primary antibodies against E-cadherin (1:200, #ab314063, Abcam) and Ki-67 (1:200, #ab16667, Abcam) at 4 °C overnight, followed by HRP-labeled secondary antibody incubation (#ab97080, Abcam) and incubated with diaminobenzidine solution and hematoxylin. Ultimately, the slides were analyzed using a light microscope (DS-U3, Nikon).

RT-qPCR assay. Total RNA of GBC cells was extracted utilizing EZ-10 Total RNA Mini-Preps Kit (#B618583-0250, BBI, Sangon Biotech, China). Next, the extracted RNA was transformed into complementary DNA (cDNA) using the TRUEscript RT MasterMix (#PC7002, Aidlab, China). Then, the RNA expression levels of circ-ZEB1, miR-144-3p, and ZEB2 were assessed using RT-qPCR with SYBR Green Mix (#PC6202, Aidlab) on a qPCR system (Roche). Primer sequences were designed and synthesized by Sangon Biotech and are listed in Table S1. Ultimately, the expressions of circ-ZEB1/ZEB2 (relative to GAPDH) and miR-144-3p (relative to U6) were analyzed by using the $2^{-\Delta\Delta Ct}$ method [21].

Western blot analysis. Total proteins of transfected GBC cells were acquired using RIPA lysis buffer (#P0013B, Beyotime) augmented with protease and phosphatase inhibitors (#P1260, Solarbio, China). The proteins were resolved by SDS-PAGE and transferred to a PVDF membrane (#10600023, GE Healthcare Life, USA). Following the use of 5% milk for blocking, the membranes were exposed to primary antibodies against E-cadherin (#20874-1-AP, 1:5000, Proteintech, China), N-cadherin (#66219-1-Ig, 1:2000, Proteintech), Slug (#AF4002, 1:1000, Affinity), ZEB2 (#AF5278, 1:1000, Affinity), and GAPDH (#10494-1-AP, 1:10000, Proteintech) overnight at 4 °C. HRP-conjugated anti-rabbit or anti-mouse antibodies (1:6000, CST) were selected as the secondary antibodies to incubate the membranes for 1 h. After that, the bands were visualized by ECL solution (#PE0010, Solarbio) and analyzed using ImageJ software (NIH, USA).

Statistical analysis. Results were shown as mean ± standard deviation (SD). All *in vitro* experiments were performed with a minimum of three independent biological replicates. The Student's t-test was employed to examine the differences between the two groups. A p-value below 0.05 was regarded as a sign of statistical significance.

Results

Upregulated circ-ZEB1 in GBC cell lines. To investigate the impact of circ-ZEB1 from ZEB1 in the development of GBC, we measured the expression levels of circ-ZEB1 in the GBC cell lines by RT-qPCR analyses. The results found that the circ-ZEB1 expression in GBC cell lines was higher than that in HGBEC cells (Figure 1A). Furthermore, inhibition of transcription using actinomycin D demonstrated that circ-ZEB1 had a notably longer half-life compared to linear ZEB1 mRNA (Figure 1B). Additionally, RNase R treatment showed resistance in circ-ZEB1, whereas linear ZEB1 mRNA showed significant degradation (Figure 1C), suggesting greater stability of the transcript. Importantly, FISH and nucleocytoplasmic fractionation assays revealed that circ-ZEB1 was localized mainly in the cytoplasm of GBC cells (Figures 1D, 1E). All in all, these findings indicated that circ-ZEB1 derived from ZEB1 as a cytoplasm-localized and stable circRNA was significantly upregulated in GBC cells.

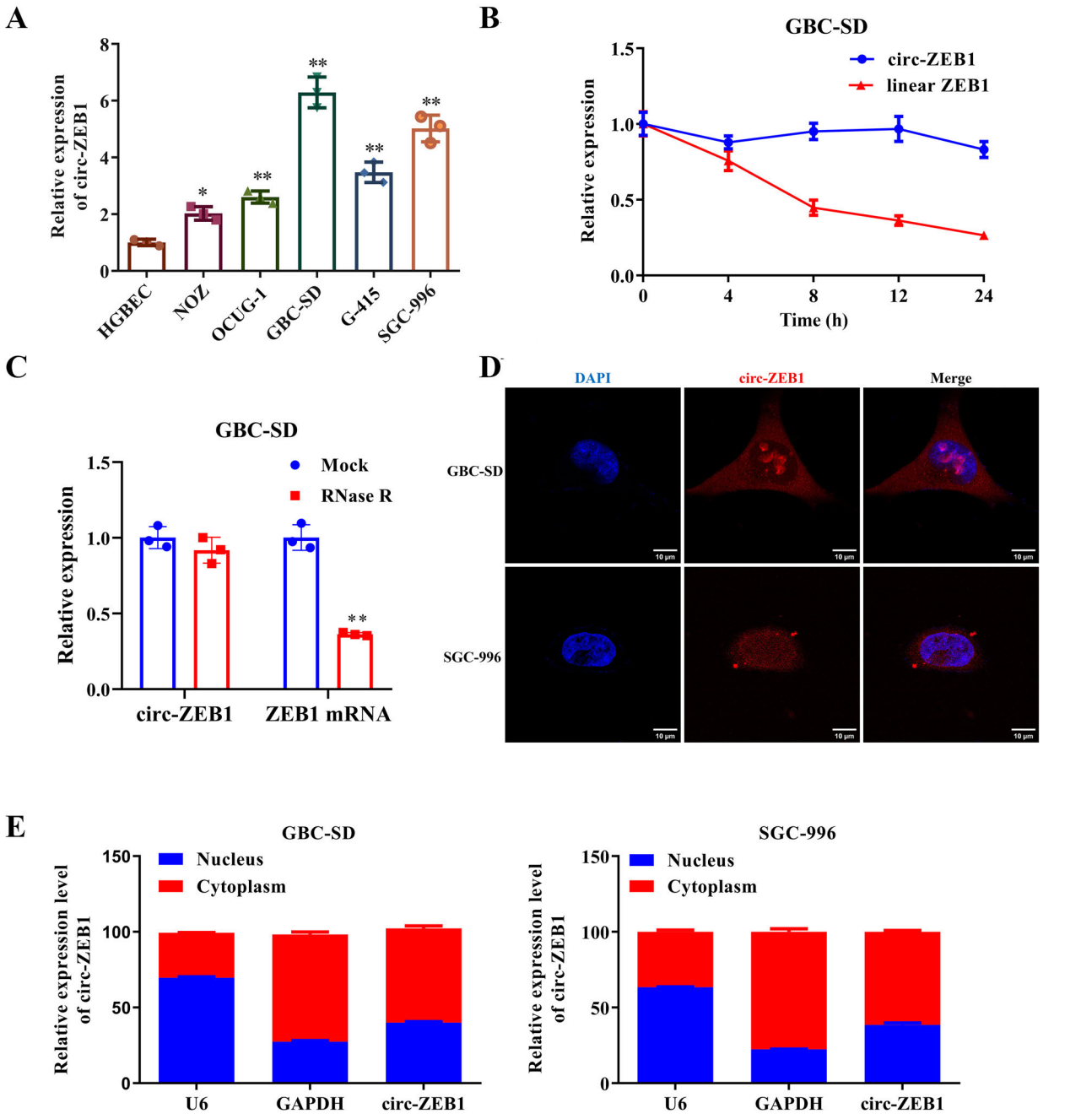

Figure 1. High expression level of circ-ZEB1 in GBC cell lines. A) Expression levels of circ-ZEB1 were detected by qRT-PCR in HGBEC cells and five GBC cell lines. B) Actinomycin D assays estimate the stability of circ-ZEB1. C) qRT-PCR displayed the expression levels of circ-ZEB1 and ZEB1 mRNA in GBC-SD cells treated with RNase R or mock control. D) RNA FISH and E) nuclear-cytoplasmic fractionation assays suggested that circ-ZEB1 is located both in the cytoplasm and nucleus of GBC cells. Scale bars = 10 μm. *p<0.05, **p<0.01

circ-ZEB1 promoted cell proliferation, migration, and invasion in GBC cells. To further explore the roles of circ-ZEB1 in GBC cells, the loss-of-function assays were conducted in GBC cells. The transfection of shRNAs targeting the back-splice region of circ-ZEB1 markedly decreased circ-ZEB1 levels in GBC cells (Figure 2A). Subsequently, CCK-8 and EdU assays showed that circ-ZEB1 inhibition significantly attenuated cell proliferation of transfected GBC cells (Figures 2B, 2C). Moreover, the Transwell cell assays showed that the silencing of circ-ZEB1 dramatically inhibited the migration and invasiveness of GBC cells (Figures 3A–3D). Interestingly, knockdown of circ-ZEB1

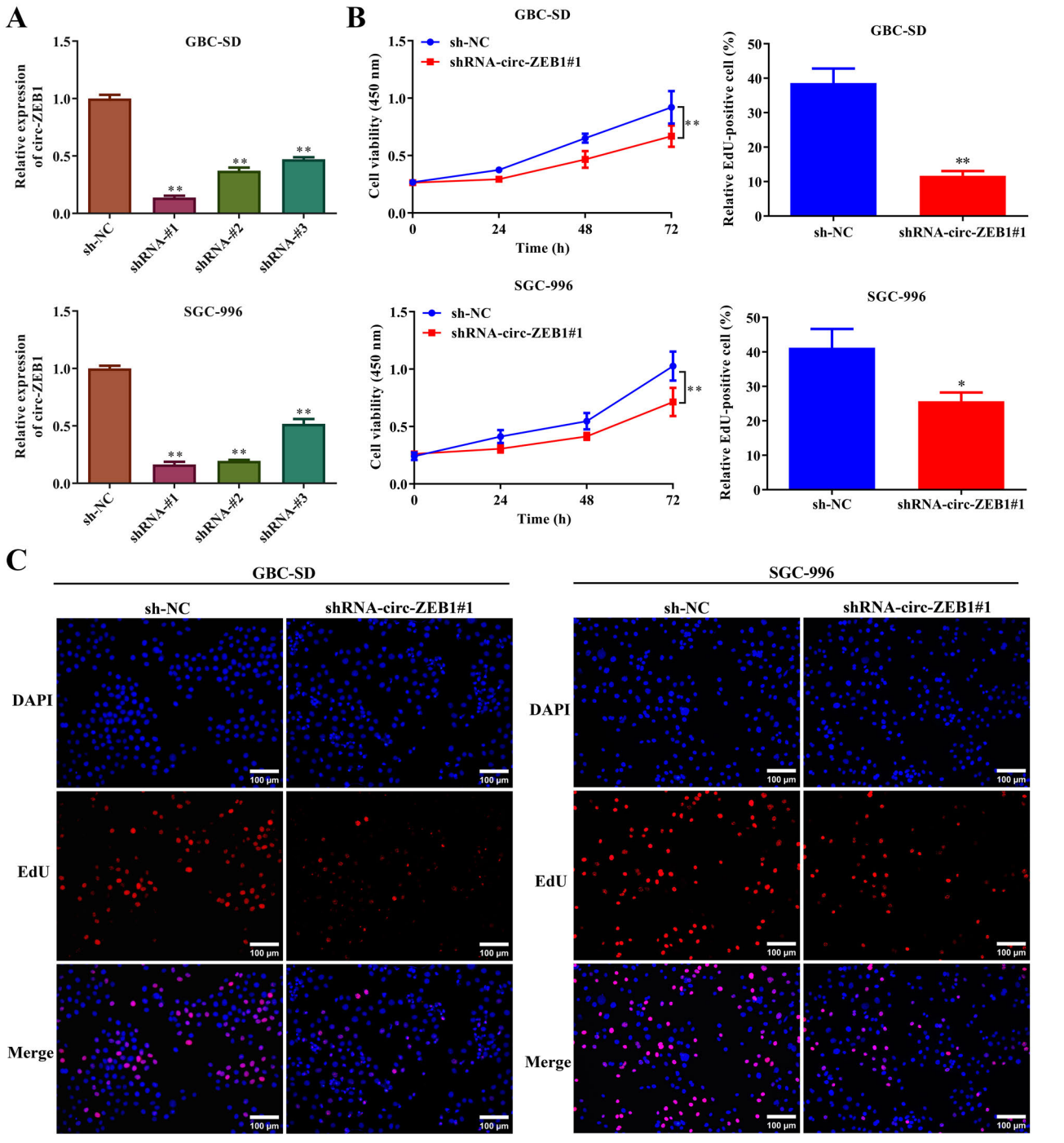

Figure 2. circ-ZEB1 knockdown inhibits cell proliferation in GBC cells. A) Relative expressions of circ-ZEB1 were measured by qRT-PCR in GBC cells transfected with shcirc-ZEB1 or sh-NC control. B) CCK-8 assay and C) EdU assay were used to detect the cell proliferation capacity of GBC cells after

reduced the protein expression levels of EMT-targets (N-cadherin and Slug), but heightened the expression of E-cadherin protein (Figures 3E, 3F). Collectively, these results illustrated that the knockdown of circ-ZEB1 depressed the malignant phenotypes of GBC cells.

circ-ZEB1 inhibition restrained tumor growth in GBC *in vivo*. A mouse model of GBC using GBC-SD cells transfected with shcirc-ZEB1 or sh-NC was developed to investigate the role of circ-ZEB1 in GBC *in vivo*. As shown in Figures 4A and 4B, circ-ZEB1 deficiency significantly diminished

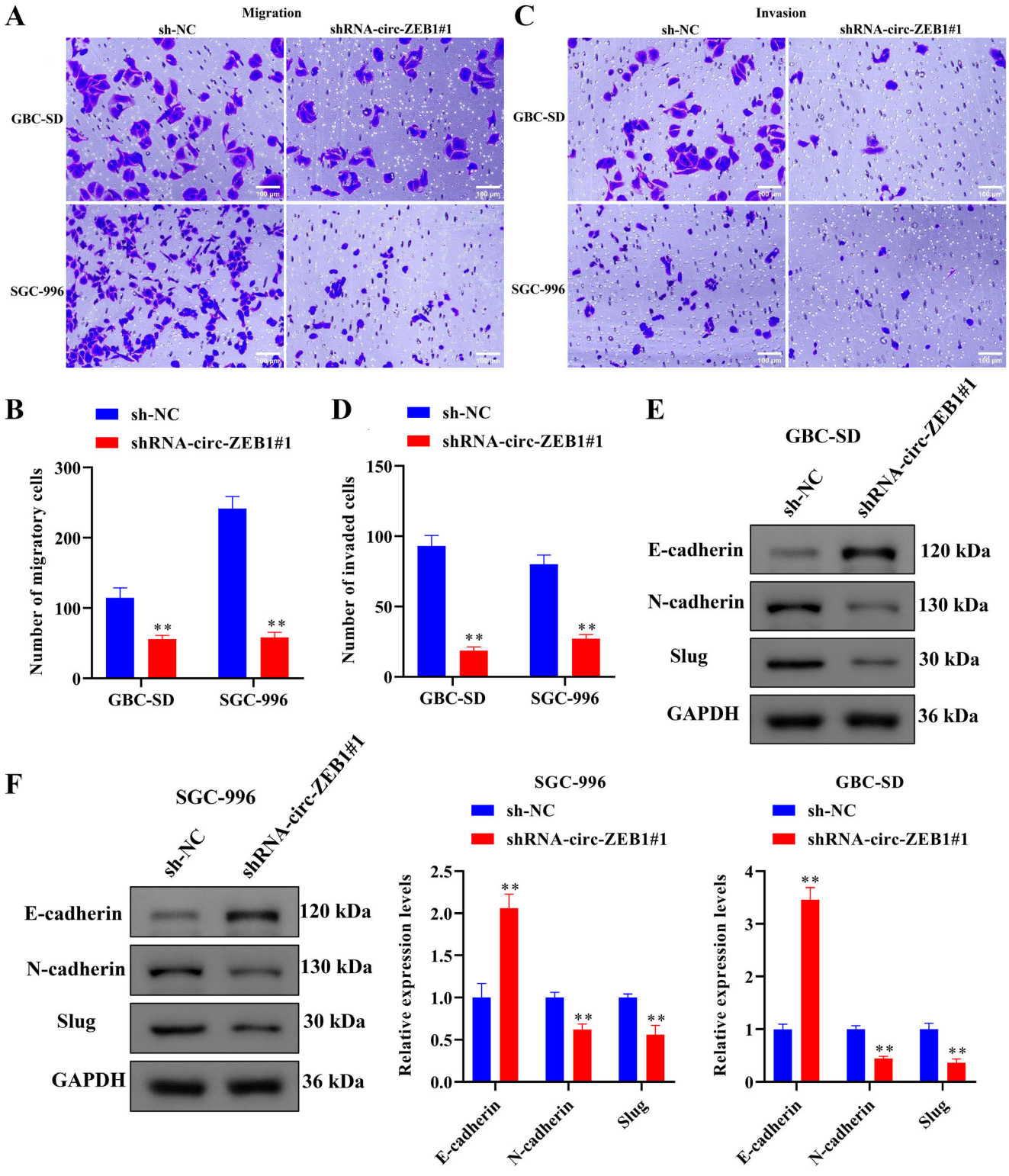

circ-ZEB1 knockdown. Scale bars = 100 μm. *p<0.05, **p<0.01

Figure 3. circ-ZEB1 knockdown attenuates the ability of cell migration and invasion in GBC cells. A–D) Transwell experiments were conducted to investigate the migration and invasion abilities of GBC cells after circ-ZEB1 knockdown. Scale bars = 100 μm. E, F) Western blot assays were performed to assess the effect of circ-ZEB1 knockdown on the expression of EMT-associated targets E-cadherin, N-cadherin, and Slug in GBC cells. *p<0.05, **p<0.01

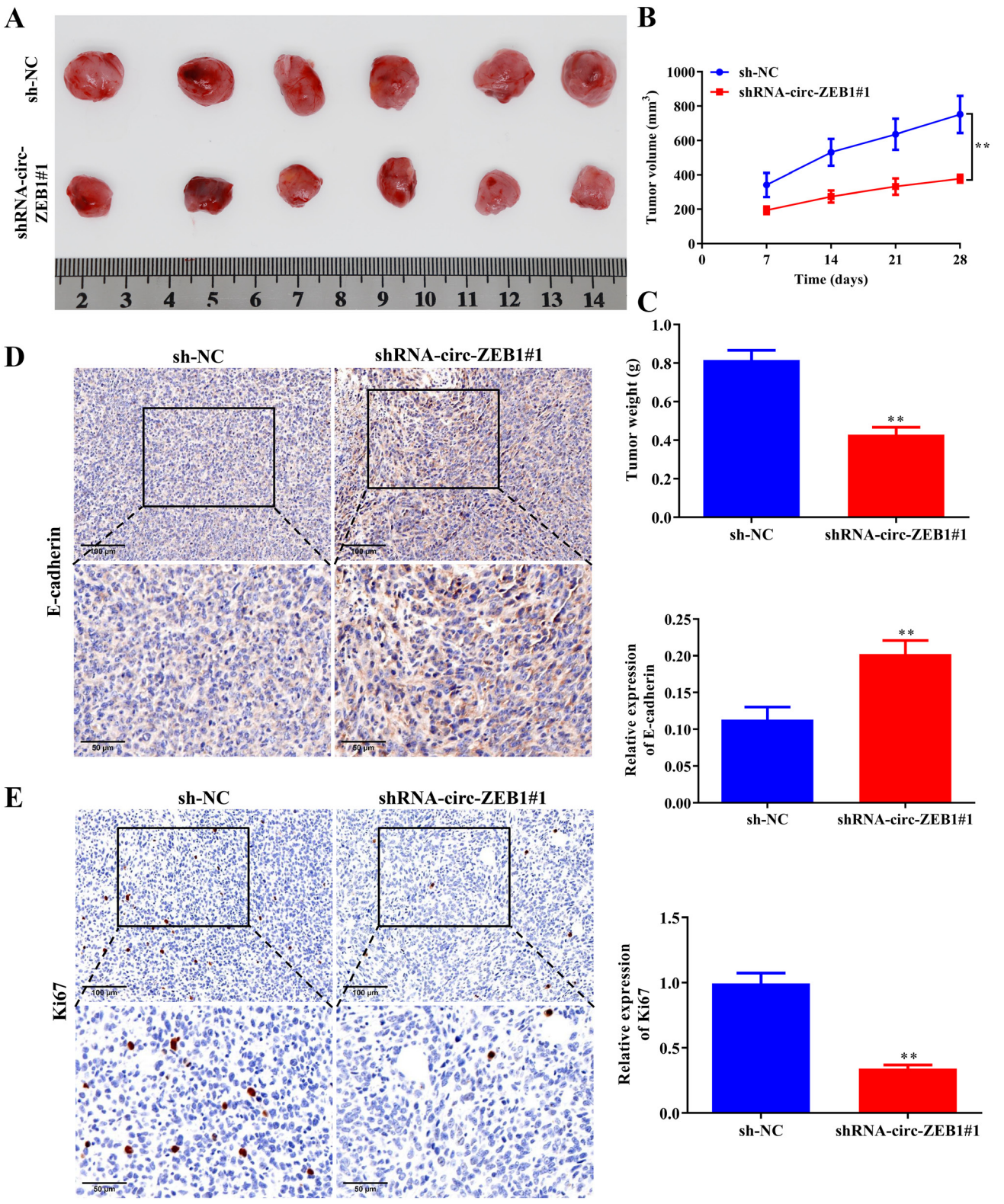

Figure 4. Effect of circ-ZEB1 knockdown on the growth of GBC cells *in vivo*. GBC-SD cells, either transfected with shcirc-ZEB1 or sh-NC, were subcutaneously administered to nude mice, and the xenograft tumors were harvested after 4 weeks. A) Representative images of xenograft tumors. B) Tumor volume was recorded every week in the nude mice. C) At the end of the experiment, the tumor weights were analyzed. D, E) IHC assays of the expression of E-cadherin and Ki-67 in tumor tissues from nude mice. Scale bars = 50 and 100 μm. *p<0.05, **p<0.01

both the tumor volume and tumor weight (Figures 4A–4C). Meanwhile, circ-ZEB1 downregulation markedly increased E-cadherin protein levels (Figure 4D) and reduced Ki-67 levels in tumor tissues (Figure 4E). In general, circ-ZEB1 deficiency contributed to inhibiting tumor growth of GBC cells *in vivo* by governing proliferation and EMT progression.

circ-ZEB1 functioned as a sponge of miR-144-3p. Considering that circ-ZEB1 was predominantly located within the cytosol, we hypothesized that it could contribute to the progression of GBC by acting as a miRNA sponge. Hence, to identify the downstream miRNAs of circ-ZEB1, the ENCORI/starBase (https://rnasysu.com/encori/) database was used. As a result, we found that circ-ZEB1 harbors potential binding sites for miR-144-3p, which formed the basis for prioritizing miR-144-3p as the focus of our subsequent research. Moreover, the luciferase activity in circ-ZEB1-wt-transfected GBC cells was decreased by miR-144-3p mimics (Figures 5A, 5B). Besides, the RIP assays showed that circ-ZEB1 and miR-144-3p were significantly enriched by the Ago2 protein in GBC cells (Figure 5C). These results indicated that circ-ZEB1 might serve as a miR-144-3p sponge to engage in the Ago2-mediated competing endogenous RNA (ceRNA) regulatory mechanism. Moreover, RT-qPCR showed lower miR-144-3p expression in GBC cell lines compared to HGBEC cells (Figure 5D). In particular, shRNA-circ-ZEB1 markedly elevated miR-144-3p levels in GBC cells (Figure 5E). These results clarify that circ-ZEB1 serves as a practical sponge for miR-144-3p in GBC cells.

miR-144-3p inhibition promoted the malignant behavior of GBC and reversed circ-ZEB1 knockdown-mediated tumor-inhibiting effects *in vitro*. To identify the function of miR-144-3p in GBC progression, the miR-144-3p inhibitor was transfected into GBC cells. The expression of miR-144-3p markedly increased in GBC cells transfected with shRNA-circ-ZEB1, while the levels of miR-144-3p were significantly decreased when treated with miR-144-3p inhibitor (Figure 6A). Importantly, the increase in miR-144-3p expression resulting from circ-ZEB1 silencing was abrogated by treatment with a miR-144-3p inhibitor (Figure 6A). Moreover, the miR-144-3p inhibitor promoted cell growth and movement of GBC-SD and SGC-996 cells. Notably, these effects were significantly counteracted by circ-ZEB1 knockdown (Figures 6B, 6C). Taken together, these results confirmed that circ-ZEB1 could develop carcinogenic effects through sponging miR-144-3p.

miR-144-3p regulated cell proliferation and migration by targeting ZEB2 in GBC cells. To analyze the subsequent targets of miR-144-3p, we identified its possible targets using TargetScan and miRDB. The results demonstrated that the ZEB2 3'-UTR had binding sites for aiming at miR-144-3p 5'-UTR (Figure 7A). As previously reported, ZEB2 functions as a transcriptional regulator that promotes EMT by repressing epithelial markers and inducing mesenchymal markers in cancers [22, 23]. However, the role and underlying mechanisms of ZEB2 in GBC have rarely been reported. Therefore, we selected ZEB2 for subsequent investigation. More importantly, the dual-luciferase assay also showed that miR-144-3p mimics decreased the luciferase activity of ZEB2-WT rather than ZEB2-Mut (Figure 7A). The expression levels of ZEB2 were significantly downregulated after silencing circ-ZEB1 expression, and the levels of ZEB2 were found to be markedly increased in GBC cells with transfection of miR-144-3p inhibitor (Figures 7B-7D). To analyze whether the miR-144-3p inhibitor promoted GBC progression by targeting ZEB2, we conducted a miR-144-3p inhibitor co-transfection with sh-ZEB2 into GBC cells. CCK-8 (Figure 7E) and Transwell assays (Figure 7F) demonstrated that ZEB2 knockdown could inhibit the malignant presentations of GBC-SD and SGC-996 cells, while the miR-144-3p inhibitor partly attenuated the effect of ZEB2 knockdown. Overall, miR-144-3p inhibited GBC cell proliferation and migration by reducing ZEB2 expression.

Discussion

GBC remains one of the most lethal forms of cancer impacting the digestive system, and the 5-year survival rate varies widely, falling between 4% and 60% [24]. The study identifies circ-ZEB1 (hsa_circ_0093509) as a cytoplasm-localized, highly stable circRNA. circ-ZEB1 is strongly upregulated in GBC. Functional and mechanistic studies show that circ-ZEB1 encourages expansion and movement, and EMT by sponging miR-144-3p, thereby relieving post-transcriptional repression of the transcription factor ZEB2. Consequently, the circ-ZEB1/miR-144-3p/ZEB2 axis constitutes a previously unrecognized oncogenic circuit in GBC and represents a potential diagnostic biomarker and therapeutic target.

circ-ZEB1 is generated from exons 2–4 of the ZEB1 gene on chr10p11.22. Consistent with previous reports in hepatocellular carcinoma [18], colorectal cancer [19], and non-small-cell lung cancer [20], we confirmed its closed-loop structure by RNase-R resistance and extended half-life by actinomycin D chase. Cytoplasmic enrichment, demonstrated by FISH and nuclear-cytoplasmic fractionation, positions circ-ZEB1 to act as a ceRNA [25, 26]. Its marked upregulation in five GBC cell lines (NOZ, OCUG-1, GBC-SD, G-415, and SGC-996) relative to HGBEC cells aligns with emerging evidence that circ-ZEB1 expression. Additionally, *in vivo*, subcutaneous xenografts derived from circ-ZEB1-silenced GBC-SD cells exhibited markedly reduced tumor volume, weight, and Ki-67 index, alongside restored E-cadherin expression, underscoring the therapeutic relevance of targeting this circRNA. Understanding the roles of circ-ZEB1 in GBC is not merely an academic exercise. The unique stability and tissue-specific expression of circRNAs make them attractive as non-invasive biomarkers detectable in plasma, bile, or exosomes [27, 28]. Moreover, recent advances in antisense oligonucleotide chemistry and CRISPR-based circular RNA editing now allow rational design of circRNA-targeted thera-

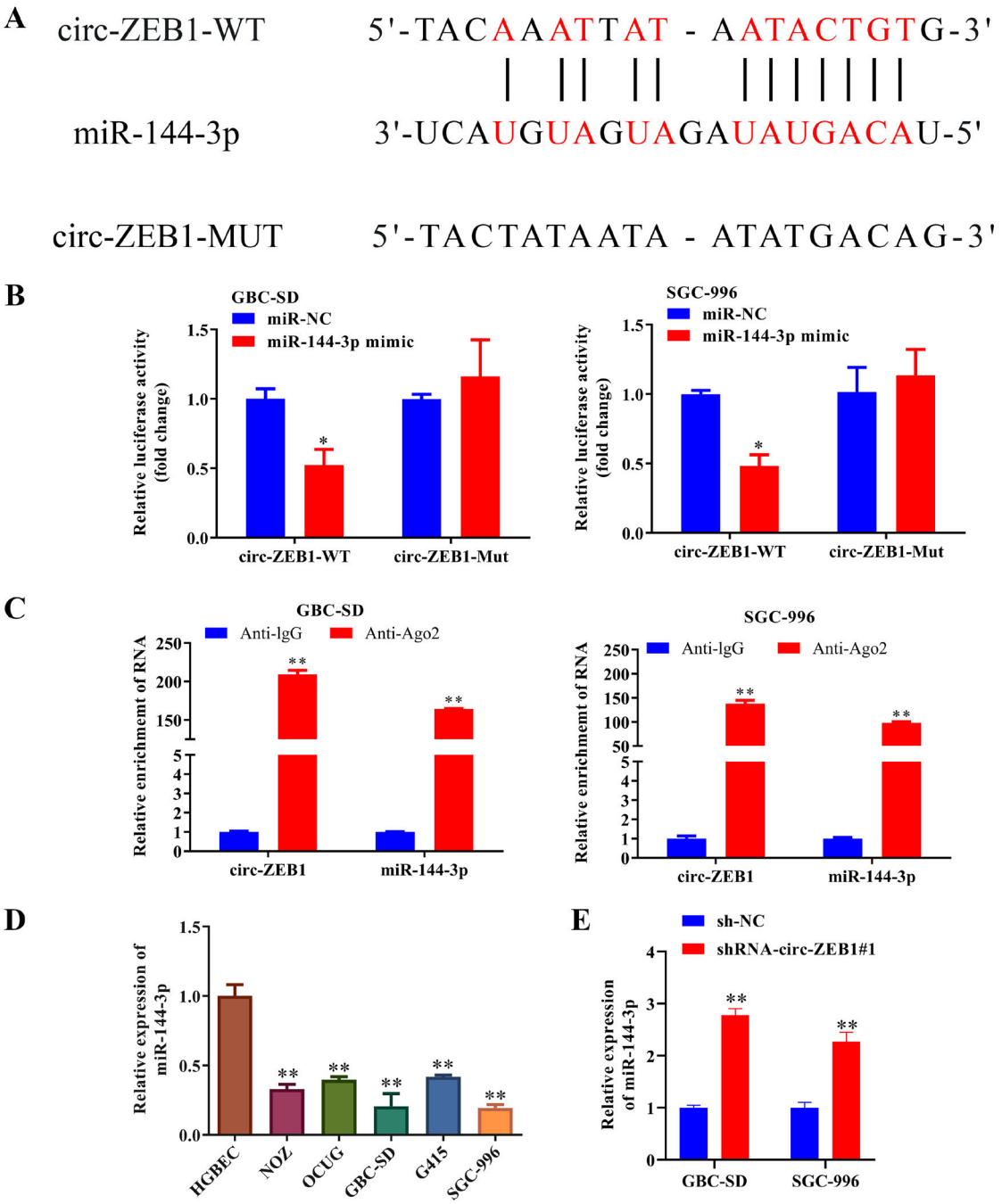

Figure 5. circ-ZEB1 could act as a miR-144-3p sponge in GBC cells. A) Predicted binding targets of circ-ZEB1 and miR-144-3p. B) Luciferase activity was measured in GBC-SD and SGC-996 cells co-transfected with circ-ZEB1-WT and circ-ZEB1-MUT with miR-144-3p mimics by using a dual-luciferase assay. C) Cell lysates of GBC-SD and SGC-996 cells were immunoprecipitated with the antibodies against IgG and Ago2, and the expression of circ-ZEB1 and miR-144-3p was detected by RT-qPCR. D) Expression levels of miR-144-3p in GBC cell lines were detected by RT-qPCR. E) Expression levels of miR-144-3p in GBC-SD and SGC-996 cells transfected with shcirc-ZEB1 or sh-NC control. *p<0.05, **p<0.01

peutics [29, 30]. If circ-ZEB1 indeed drives GBC progression, it may act as both a predictive biomarker for early detection and a tractable therapeutic target to overcome the notorious chemoresistance that characterizes this illness.

Mechanistically, circ-ZEB1 sequesters miR-144-3p through direct binding sites, as confirmed by the Ago2-RIP assay. miR-144-3p is a well-documented tumor suppressor whose loss is associated with invasion and metastasis in

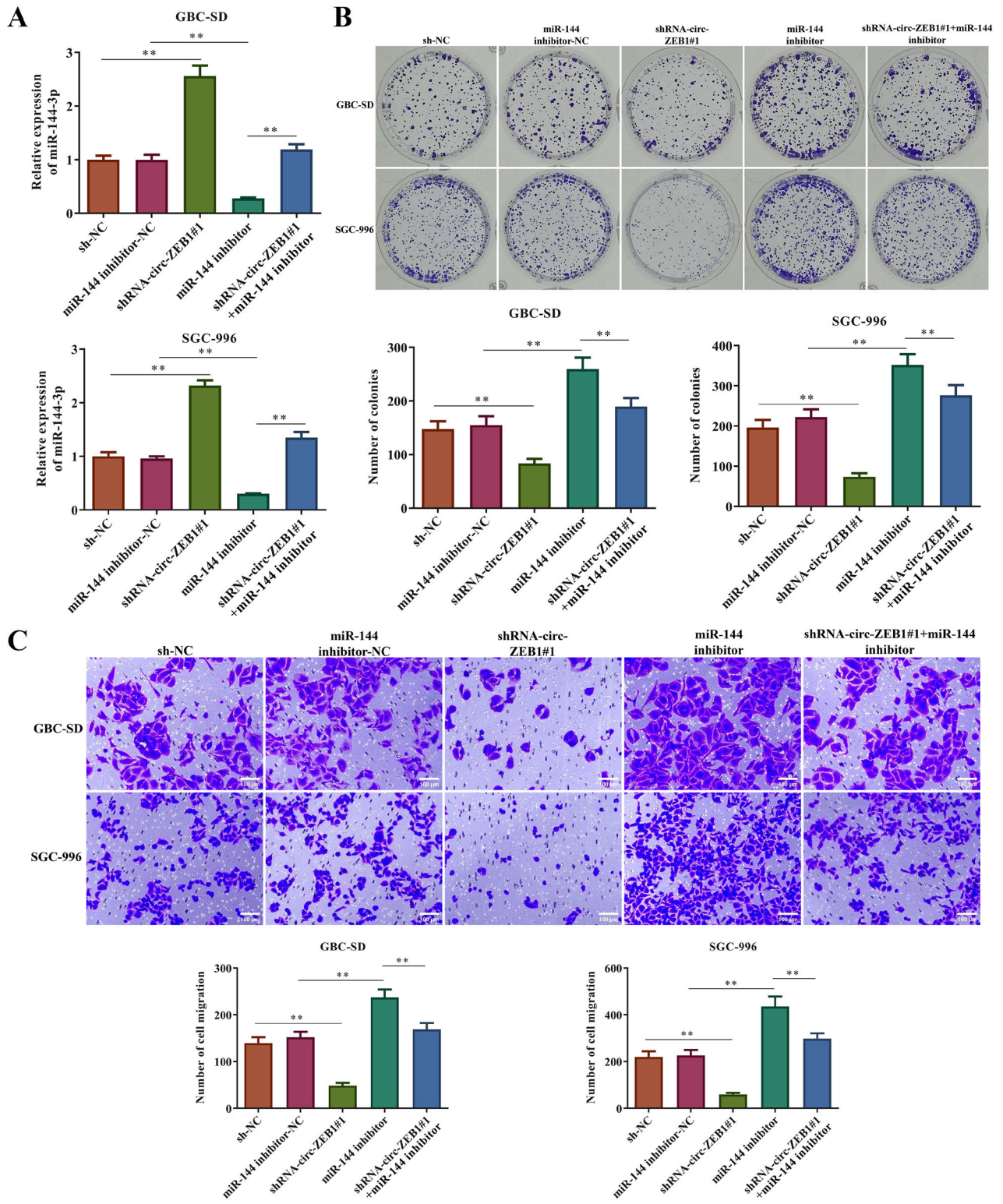

Figure 6. miR-144-3p silencing attenuated circ-ZEB1 knockdown-induced inhibition of proliferation and migration in GBC-SD and SGC-996 cells. A) Relative expressions of miR-144-3p in GBC-SD and SGC-996 cells co-transfected with shcirc-ZEB1 and miR-144-3p inhibitor alone or in combination were detected by RT-qPCR. B) Colony formation assay was used to assess the GBC-SD and SGC-996 cellular proliferation when transfected with sh-NC, miR-144-3p inhibitor-NC, shRNA-circ-ZEB1#1, miR-144-3p inhibitor, and shRNA-circ-ZEB1#1+miR-144-3p inhibitor. C) Transwell migration assay was utilized to analyze the migration of GBC-SD and SGC-996 cells when transfected with sh-NC, miR-144-3p inhibitor-NC, shRNA-circ-ZEB1#1, miR-144-3p inhibitor, and shRNA-circ-ZEB1#1+miR-144-3p inhibitor. Scale bars = 100 μm. **p<0.01

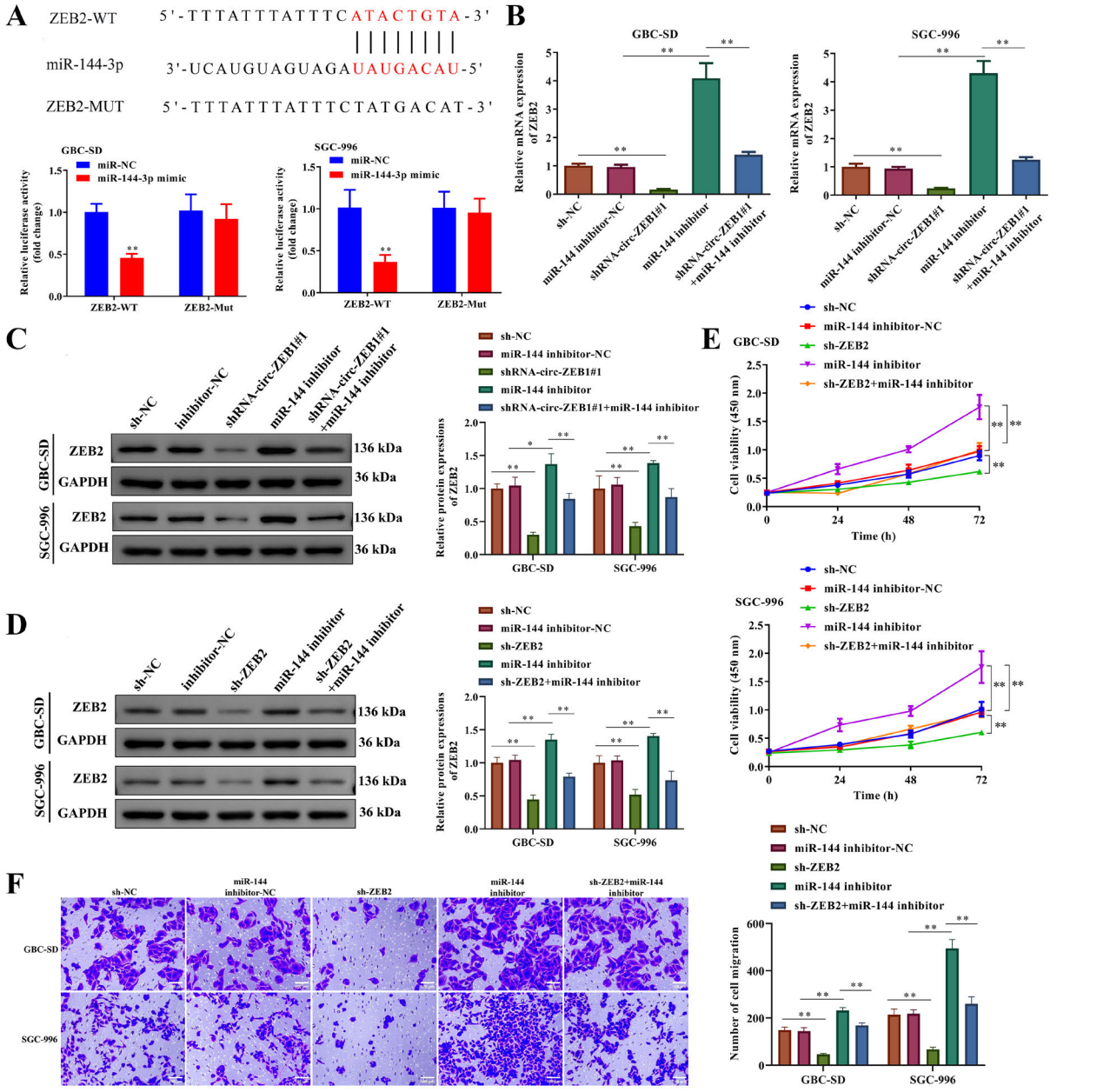

Figure 7. miR-144-3p targets ZEB2, and miR-144-3p inhibition attenuates the inhibitory effect of ZEB1 knockdown on GBC cells. A) The predicted binding sites between ZEB2 and miR-144-3p were exhibited, and the dual luciferase reporter assays were performed to investigate whether ZEB2 could bind to miR-144-3p. B) RT-qPCR analysis was used to measure expression levels of ZEB2 in GBC-SD and SGC-996 cells when transfected with sh-NC, miR-144-3p inhibitor-NC, shRNA-circ-ZEB1#1, miR-144-3p inhibitor, and shRNA-circ-ZEB1#1+miR-144-3p inhibitor. C, D) Western blot assays measured the ZEB2 protein expression in GBC-SD and SGC-996 cells transfected with sh-NC, miR-144-3p inhibitor-NC, shRNA-circ-ZEB1#1, sh-ZEB2, miR-144-3p inhibitor, shRNA-circ-ZEB1#1+miR-144-3p inhibitor, and sh-ZEB2+miR-144-3p inhibitor. E, F) CCK-8 and Transwell migration assays were employed to assess the malignant phenotypes of GBC-SD and SGC-996 cells when transfected with sh-NC, miR-144-3p inhibitor-NC, sh-ZEB2, miR-144-3p inhibitor, and sh-ZEB2+miR-144-3p inhibitor. Scale bars = 100 μm. *p<0.05, **p<0.01

thyroid cancer [31] and gastric cancer [32]. Our data extend these observations to GBC, showing that miR-144-3p directly targets the 3'-UTR of ZEB2 mRNA, thereby reducing its expression. ZEB2, an important component of the ZEB family, functions as a transcriptional repressor that regulates EMT by interacting with E-box elements present in the promoter of E-cadherin [33]. In hepatocellular carcinoma, ZEB2 overexpression correlates with vascular invasion and poor prognosis [34]. Similarly, in colorectal carcinoma, a ZEB2-mediated EMT program underlies metastasis [35].

In breast cancer, ZEB2 cooperates with ACSL4 signaling to promote lipid droplet storage and tumor progression [36]. Our findings now add GBC to this list, demonstrating that ZEB2 upregulation via circ-ZEB1/miR-144-3p sequestration is sufficient to accelerate malignant behavior. Importantly, ZEB2 expression is also regulated by DNA methylation [37] and deubiquitination [38], suggesting that integrating circRNA-based and epigenetic strategies could enhance therapeutic efficacy.

However, there are some shortcomings in this study. First, the study relied on two GBC cell lines and a subcutaneous xenograft model; validation in patient-derived organoids and orthotopic or genetically engineered mouse models is warranted. Second, circ-ZEB1 may interact with additional miRNAs or RNA-binding proteins that were not interrogated. Third, the expression of circ-ZEB1 should be verified in patient tissue specimens to enhance its clinical value, and the clinical translation requires prospective cohorts to assess circ-ZEB1 levels in bile or plasma as non-invasive biomarkers. Finally, therapeutic targeting of circ-ZEB1 via antisense oligonucleotides or CRISPR-based circular RNA editing must address delivery specificity and off-target effects.

In summary, we identify circ-ZEB1 as a key oncogenic circRNA that promotes GBC progression via the miR-144-3p/ZEB2 axis. By sponging miR-144-3p, circ-ZEB1 unleashes ZEB2 to drive EMT, proliferation, and metastasis. This axis-conserved yet contextually pivotal in GBC represents a promising therapeutic target. Future work should prioritize clinical validation and RNA-based therapeutic development to combat this lethal malignancy.

Supplementary information is available in the online version of the paper.

Acknowledgments: This work was supported by The Technology Plan Project of Taizhou (No. 24ywb79) and Medical Health Science and Technology Project of Zhejiang Provincial Health Commission (No. 2022KY1397).

References

[1] LIU Q, ZHANG P, LI Q. Exploring Molecular Mechanisms in the Second-Line Treatment of Biliary Tract Malignant Tumors. Discov Med 2024; 36: 48–60. https://doi.org/10.24976/Discov.Med.202436180.4

[2] BURUD IA, ELHARIRI S, EID N. Gallbladder carcinoma in the era of artificial intelligence: Early diagnosis for better treatment. World J Gastrointest Oncol 2025; 17: 99994. https://doi.org/10.4251/wjgo.v17.i1.99994

[3] SHAHIN RK, ELKADY MA, ABULSOUD AI, ABDELMAKSOUD NM, ABDEL MAGEED SS et al. miRNAs orchestration of gallbladder cancer – Particular emphasis on diagnosis, progression and drug resistance. Pathol Res Pract 2023; 248: 154684. https://doi.org/10.1016/j.prp.2023.154684

[4] SIEGELRL, MILLER KD, FUCHS HE, JEMAL A. Cancer Statistics, 2021. CA Cancer J Clin 2021; 71: 7–33. https://doi.org/10.3322/caac.21654

[5] BOJAN A, PRICOP C, VLADEANU MC, BARARU-BOJAN I, HALITCHI CO et al. The Predictive Roles of Tumour Markers, Hemostasis Assessment, and Inflammation in the Early Detection and Prognosis of Gallbladder Adenocarcinoma and Metaplasia: A Clinical Study. Int J Mol Sci 2025; 26: 3665. https://doi.org/10.3390/ijms26083665

[6] VUTHALURU S, SHARMA P, CHOWDHURY S, ARE C. Global epidemiological trends and variations in the burden of gallbladder cancer. J Surg Oncol 2023; 128: 980–988. https://doi.org/10.1002/jso.27450

[7] PATKAR S, PATEL S, KAZI M, GOEL M. Radical surgery for stage IV gallbladder cancers: Treatment strategies in patients with limited metastatic burden. Ann Hepatobiliary Pancreat Surg. 2023; 27: 180–188. https://doi.org/10.14701/ahbps.22-111

[8] KRISTENSEN LS, ANDERSEN MS, STAGSTED LVW, EBBESEN KK, HANSEN TB et al. The biogenesis, biology and characterization of circular RNAs. Nat Rev Genet 2019; 20: 675–691. https://doi.org/10.1038/s41576-019-0158-7

[9] ZHANG W, XU C, YANG Z, ZHOU J, PENG W et al. Circular RNAs in tumor immunity and immunotherapy. Mol Cancer 2024; 23: 171. https://doi.org/10.1186/s12943-024-02082-z

[10] LIU X, ZHANG Y, ZHOU S, DAIN L, MEI L et al. Circular RNA: An emerging frontier in RNA therapeutic targets, RNA therapeutics, and mRNA vaccines. J Control Release 2022; 348: 84–94. https://doi.org/10.1016/j.jconrel.2022.05.043

[11] WU Y, WANG F, SHI J, GUO X, LI F. CircSMAD2 accelerates endometrial cancer cell proliferation and metastasis by regulating the miR-1277-5p/MFGE8 axis. J Gynecol Oncol 2023; 34: e19. https://doi.org/10.3802/jgo.2023.34.e19

[12] LIU CX, CHEN LL. Circular RNAs: Characterization, cellular roles, and applications. Cell 2022; 185: 2016–2034. https://doi.org/10.1016/j.cell.2022.04.021

[13] HU B, YANG H, WANG Y, CAO Y, ZHOU R et al. Downregulated circRNA_CDKN1A promotes gallbladder cancer progression through activation of the NF-κB pathway. Cell Biochem Funct 2024; 42: e3952. https://doi.org/10.1002/cbf.3952

[14] QIN Y, ZHENG Y, HUANG C, LI Y, GU M et al. Knockdown of circSMAD2 inhibits the tumorigenesis of gallbladder cancer through binding with eIF4A3. BMC Cancer 2021; 21: 1172. https://doi.org/10.1186/s12885-021-08895-1

[15] LIU S, WANG Y, WANG T, SHI K, FAN S et al. CircPCNXL2 promotes tumor growth and metastasis by interacting with STRAP to regulate ERK signaling in intrahepatic cholangiocarcinoma. Mol Cancer 2024; 23: 35. https://doi.org/10.1186/s12943-024-01950-y

[16] CHENG L, ZHOU MY, GU YJ, CHEN L, WANG Y. ZEB1: New advances in fibrosis and cancer. Mol Cell Biochem 2021; 476: 1643–1650. https://doi.org/10.1007/s11010-020-04036-7

[17] KINOUCHI A, JUBASHI T, TATSUNO R, ICHIKAWA J, SAKAMOTO K et al. Roles of ZEB1 and ZEB2 in E-cadherin expression and cell aggressiveness in head and neck cancer. Genes Cells 2024; 29: 1131–1143. https://doi.org/10.1111/gtc.13167

[18] LIU W, ZHENG L, ZHANG R, HOU P, WANG J et al. Circ-ZEB1 promotes PIK3CA expression by silencing miR-199a-3p and affects the proliferation and apoptosis of hepatocellular carcinoma. Mol Cancer 2022; 21: 72. https://doi.org/10.1186/s12943-022-01529-5

[19] CHEN H, ZHANG J, YANG L, LI Y, WANG Z et al. circ-ZEB1 regulates epithelial-mesenchymal transition and chemotherapy resistance of colorectal cancer through acting on miR-200c-5p. Transl Oncol 2023; 28: 101604. https://doi.org/10.1016/j.tranon.2022.101604

[20] WANG Q, LING S, LV J, WU L. circ-ZEB1 Enhances NSCLC Metastasis and Proliferation by Modulating the miR-491-5p/EIF5A Axis. Anal Cell Pathol (Amst) 2025; 2025:5595692. https://doi.org/10.1155/ancp/5595692

[21] LIVAK KJ, SCHMITTGEN TD. Analysis of relative gene expression data using real-time quantitative PCR and the 2(–Delta Delta C(T)) Method. Methods 2001; 25: 402–408. https://doi.org/10.1006/meth.2001.1262

[22] ANG HL, MOHAN CD, SHANMUGAM MK, LEONG HC, MAKVANDI P et al. Mechanism of epithelial-mesenchymal transition in cancer and its regulation by natural compounds. Med Res Rev 2023; 43: 1141–1200. https://doi.org/10.1002/med.21948

[23] GHAFOOR S, GARCIA E, JAY DJ, PERSAD S. Molecular Mechanisms Regulating Epithelial Mesenchymal Transition (EMT) to Promote Cancer Progression. Int J Mol Sci. 2025; 26: 4364. https://doi.org/10.3390/ijms26094364

[24] RODAS F, VIDAL-VIDAL JA, HERRERA D, BROWN-BROWN DA, VERA D et al. Targeting the Endothelin-1 pathway to reduce invasion and chemoresistance in gallbladder cancer cells. Cancer Cell Int 2023; 23: 318. https://doi.org/10.1186/s12935-023-03145-9

[25] YANG S, WANG X, ZHOU X, HOU L, WU J et al. ncRNA-mediated ceRNA regulatory network: Transcriptomic insights into breast cancer progression and treatment strategies. Biomed Pharmacother 2023; 162: 114698. https://doi.org/10.1016/j.biopha.2023.114698

[26] WU S, ZHONG B, YANG Y, WANG Y, PAN Z. ceRNA networks in gynecological cancers progression and resistance. J Drug Target 2023; 31: 920–930. https://doi.org/10.1080/1061186X.2023.2261079

[27] KRISTENSEN LS, JAKOBSEN T, HAGER H, KJEMS J. The emerging roles of circRNAs in cancer and oncology. Nat Rev Clin Oncol 2022; 19: 188–206. https://doi.org/10.1038/s41571-021-00585-y

[28] LI C, NI YQ, XU H, XIANG QY, ZHAO Y et al. Roles and mechanisms of exosomal non-coding RNAs in human health and diseases. Signal Transduct Target Ther 2021; 6: 383. https://doi.org/10.1038/s41392-021-00779-x

[29] HE AT, LIU J, LI F, YANG BB. Targeting circular RNAs as a therapeutic approach: current strategies and challenges. Signal Transduct Target Ther 2021; 6: 185. https://doi.org/10.1038/s41392-021-00569-5

[30] MAGOOLA M, NIAZI SK. Current Progress and Future Perspectives of RNA-Based Cancer Vaccines: A 2025 Update. Cancers (Basel) 2025; 17: 1882. https://doi.org/10.3390/cancers17111882

[31] XIU C, DENG X, DENG D, ZHOU T, JIANG C et al. miR-144-3p Targets GABRB2 to Suppress Thyroid Cancer Progression In Vitro. Cell Biochem Biophys 2024; 82: 3585–3595. https://doi.org/10.1007/s12013-024-01446-y

[32] LU Y, ZHANG B, WANG B, WU D, WANG C et al. MiR-144-3p inhibits gastric cancer progression and stemness via directly targeting GLI2 involved in hedgehog pathway. J Transl Med 2021; 19: 432. https://doi.org/10.1186/s12967-021-03093-w

[33] KOOPMANSCH B, BERX G, FOIDART JM, GILLES C, WINKLER R. Interplay between KLF4 and ZEB2/SIP1 in the regulation of E-cadherin expression. Biochem Biophys Res Commun 2013; 431: 652–657. https://doi.org/10.1016/j.bbrc.2013.01.070

[34] GAO HB, GAO FZ, CHEN XF. MiRNA-1179 suppresses the metastasis of hepatocellular carcinoma by interacting with ZEB2. Eur Rev Med Pharmacol Sci 2019; 23: 5149–5157. https://doi.org/10.26355/eurrev_201906_18179

[35] ZHENG Y, DAI M, DONG Y, YU H, LIU T et al. ZEB2/TWIST1/PRMT5/NuRD Multicomplex Contributes to the Epigenetic Regulation of EMT and Metastasis in Colorectal Carcinoma. Cancers (Basel) 2022; 14: 3426. https://doi.org/10.3390/cancers14143426

[36] LIN J, ZHANG P, LIU W, LIU G, ZHANG J et al. A positive feedback loop between ZEB2 and ACSL4 regulates lipid metabolism to promote breast cancer metastasis. Elife 2023; 12: RP87510. https://doi.org/10.7554/eLife.87510

[37] XIE H, WU Z, LI Z, HUANG Y, ZOU J et al. Significance of ZEB2 in the immune microenvironment of colon cancer. Front Genet 2022; 13: 995333. https://doi.org/10.3389/fgene.2022.995333

[38] ZHANG L, XU J, ZHOU S, YAO F, ZHANG R et al. Endothelial DGKG promotes tumor angiogenesis and immune evasion in hepatocellular carcinoma. J Hepatol 2024; 80: 82–98. https://doi.org/10.1016/j.jhep.2023.10.006

https://doi.org/10.4149/neo_2026_251124N495

circRNA circ-ZEB1 promotes gallbladder carcinomas progression by regulating the miR-144-3p/ZEB2 axis

Luoshun HUANG#, Yang ZHANG#, Fan YANG, Yisheng LING, Xianfei ZHOU*

Supplementary Information

Supplementary Table S1. Sequences of shRNA and qRT-PCR primers.

Targets	Sequences (5'–3')	Product length
sh-circ-ZEB1-#1	5'-ATAGAAGACCATGGATCATTG-3'	/
sh-circ-ZEB1-#2	5'-CAGTAATATTCCATCATATTC-3'	/
sh-circ-ZEB1-#3	5'-TCAGGTCCTACTTATACTCAA-3'	/
sh-ZEB2-#1	5'-CTAGACTTCAATGACTATAAA-3'	/
sh-ZEB2-#2	5'-CACGATCCAGACCGCAATTAA-3'	/
sh-ZEB2-#3	5'-CAGTGACACAGCCATTATTTA-3'	/
miR-144-3p inhibitor	5'-AGTACATCATCTATACTGTA-3'	/
circ-ZEB1	Forward, 5-CCTGTGCAGTTACACCTTTGC-3' Reverse, 5'-TTGCCCTTCCTTTCCTGTGT-3'	400 bp
miR-144-3p	Forward, 5'-GCGCGCTACAGTATAGATGA-3' Reverse, 5'-GTGCAGGGTCCGAGGT-3'	/
ZEB1	Forward, 5'-GAGCAGCCTAGCCAACTTCA-3' Reverse, 5'-GGAGTGGAGGAGGCTGAGTA-3'	247 bp
ZEB2	Forward, 5'-AGCCTCTGTAGATGGTCCAGT-3' Reverse, 5'-GGTCAGCAGTTGGGCAAAAG-3'	253 bp
GAPDH	Forward, 5'-GAAGGTGAAGGTCGGAGTC-3' Reverse, 5'-GAAGATGGTGATGGGATTTC-3'	226 bp
U6	Forward, 5'-CTCGCTTCGGCAGCACA-3' Reverse, 5'-AACGCTTCACGAATTTGCGT-3'	/

The circ-ZEB1 sequence along with an indication of the sequences recognized by the primers

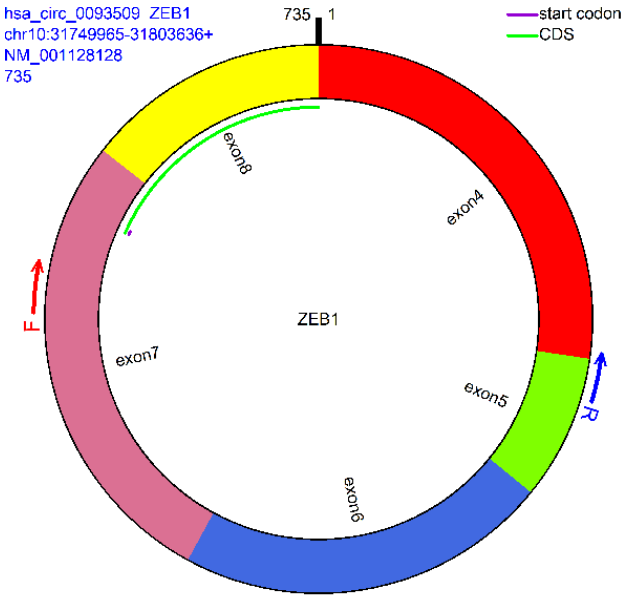

Schematic diagram showing the location of primers in the circular RNA

The sequence of the circ-ZEB1 backs plice junction used in the luciferase reporter constructs

>hsa_circ_0093509:
TTACAAATTATAATACTGTGGTAGAAACAAATTCAGATTCAGATGATGAAGACAAACTGC
ATATTGTGGAAGAAGAAAGTGTTACAGATGCAGCTGACTGTGAAGGTGTACCAGAGGAT
GACCTGCCAACAGACCAGACAGTGTTACCAGGGAGGAGCAGTGAAAGAGAAGGGAAT
GCTAAGAACTGCTGGGAGGATGACACAGGAAAGGAAGGGCAAGAAATCCTGGGGCCT
GAAGCTCAGGCAGATGAAGCAGGATGTACAGTAAAAGATGATGAATGCGAGTCAGATG
CAGAAAATGAGCAAAACCATGATCCTAATGTTGAAGAGTTTCTACAACAACAAGACACT
GCTGTCATTTTTCCTGAGGCACCTGAAGAGGACCAGAGGCAGGGCACACCAGAAGCCA
GTGGTCATGATGAAAATGGAACACCAGATGCATTTTCACAATTACTCACCTGTCCATATT
GTGATAGAGGCTATAAACGCTTTACCTCTCTGAAAGAACACATTAAATATCGTCATGAAA
AGAATGAAGATAACTTTAGTTGCTCCCTGTGCAGTTACACCTTTGCATACAGAACCCAAC
TTGAACGTCACATGACATCACATAAATCAGGAAGAGATCAAAGACATGTGACGCAGTCT
GGGTGTAATCGTAAATTCAAATGCACTGAGTGTGGAAAAGCTTTCAAATACAAACATCA
CCTAAAAGAGCACTTAAGAATTCACAGTG

>hsa-miR-144-3p:
UACAGUAUAGAUGAUGUACU

Forward: Score: 151.000000 Q:2 to 18 R:2 to 20 Align Len (16) (75.00%) (81.25%)

Query: 3' ucaUGUAGUAGAUAUGACAu 5'

| ||:|| |||||||

Ref: 5' tacAAATTAT-AATACTGTg 3'

Energy: -12.010000 kCal/Mol

Scores for this hit:
>hsa-miR-144-3p: hsa_circ_0093509: 151.00 -12.01 2 18 2 20 16 75.00% 81.25%

The binding site is located relatively upstream. Since the target gene is a circular RNA, a sequence was taken from the end and appended to the front to design the wild-type and mutant constructs.

>hsa_circ_0093509 WT-hsa-miR-144-3p:
AGAGCACTTAAGAATTCACAGTGTTACAAATTATAATACTGTGGTAGAAACAAATTCAGA
TTCAGATGAT
>hsa_circ_0093509 MUT-hsa-miR-144-3p:
AGAGCACTTAAGAATTCACAGTGTTACTATAATAATATGACAGGTAGAAACAAATTCAGA
TTCAGATGAT

https://doi.org/10.4149/neo_2026_251124N495

circRNA circ-ZEB1 promotes gallbladder carcinomas progression by regulating the miR-144-3p/ZEB2 axis

Luoshun HUANG#, Yang ZHANG#, Fan YANG, Yisheng LING, Xianfei ZHOU*

Supplementary Information

Supplementary Table S1. Sequences of shRNA and qRT-PCR primers.

Targets	Sequences (5'–3')	Product length
sh-circ-ZEB1-#1	5'-ATAGAAGACCATGGATCATTG-3'	/
sh-circ-ZEB1-#2	5'-CAGTAATATTCCATCATATTC-3'	/
sh-circ-ZEB1-#3	5'-TCAGGTCCTACTTATACTCAA-3'	/
sh-ZEB2-#1	5'-CTAGACTTCAATGACTATAAA-3'	/
sh-ZEB2-#2	5'-CACGATCCAGACCGCAATTAA-3'	/
sh-ZEB2-#3	5'-CAGTGACACAGCCATTATTTA-3'	/
miR-144-3p inhibitor	5'-AGTACATCATCTATACTGTA-3'	/
circ-ZEB1	Forward, 5-CCTGTGCAGTTACACCTTTGC-3' Reverse, 5'-TTGCCCTTCCTTTCCTGTGT-3'	400 bp
miR-144-3p	Forward, 5'-GCGCGCTACAGTATAGATGA-3' Reverse, 5'-GTGCAGGGTCCGAGGT-3'	/
ZEB1	Forward, 5'-GAGCAGCCTAGCCAACTTCA-3' Reverse, 5'-GGAGTGGAGGAGGCTGAGTA-3'	247 bp
ZEB2	Forward, 5'-AGCCTCTGTAGATGGTCCAGT-3' Reverse, 5'-GGTCAGCAGTTGGGCAAAAG-3'	253 bp
GAPDH	Forward, 5'-GAAGGTGAAGGTCGGAGTC-3' Reverse, 5'-GAAGATGGTGATGGGATTTC-3'	226 bp
U6	Forward, 5'-CTCGCTTCGGCAGCACA-3' Reverse, 5'-AACGCTTCACGAATTTGCGT-3'	/

The circ-ZEB1 sequence along with an indication of the sequences recognized by the primers

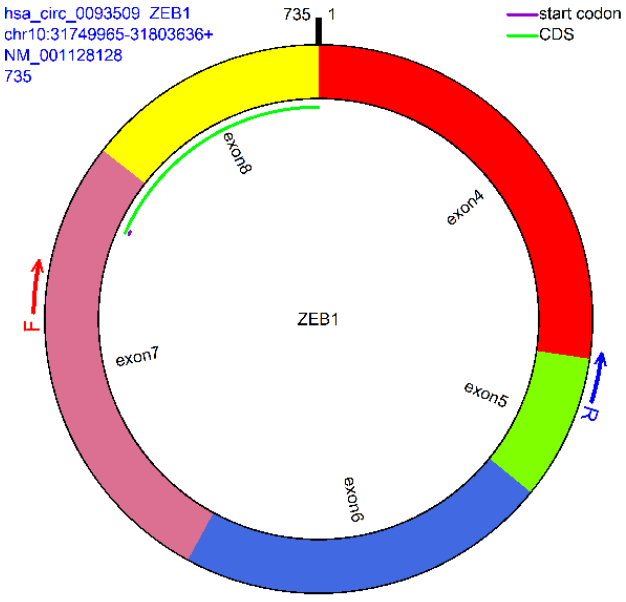

Schematic diagram showing the location of primers in the circular RNA

The sequence of the circ-ZEB1 backs plice junction used in the luciferase reporter constructs

>hsa_circ_0093509:
TTACAAATTATAATACTGTGGTAGAAACAAATTCAGATTCAGATGATGAAGACAAACTGC
ATATTGTGGAAGAAGAAAGTGTTACAGATGCAGCTGACTGTGAAGGTGTACCAGAGGAT
GACCTGCCAACAGACCAGACAGTGTTACCAGGGAGGAGCAGTGAAAGAGAAGGGAAT
GCTAAGAACTGCTGGGAGGATGACACAGGAAAGGAAGGGCAAGAAATCCTGGGGCCT
GAAGCTCAGGCAGATGAAGCAGGATGTACAGTAAAAGATGATGAATGCGAGTCAGATG
CAGAAAATGAGCAAAACCATGATCCTAATGTTGAAGAGTTTCTACAACAACAAGACACT
GCTGTCATTTTTCCTGAGGCACCTGAAGAGGACCAGAGGCAGGGCACACCAGAAGCCA
GTGGTCATGATGAAAATGGAACACCAGATGCATTTTCACAATTACTCACCTGTCCATATT
GTGATAGAGGCTATAAACGCTTTACCTCTCTGAAAGAACACATTAAATATCGTCATGAAA
AGAATGAAGATAACTTTAGTTGCTCCCTGTGCAGTTACACCTTTGCATACAGAACCCAAC
TTGAACGTCACATGACATCACATAAATCAGGAAGAGATCAAAGACATGTGACGCAGTCT
GGGTGTAATCGTAAATTCAAATGCACTGAGTGTGGAAAAGCTTTCAAATACAAACATCA
CCTAAAAGAGCACTTAAGAATTCACAGTG

>hsa-miR-144-3p:
UACAGUAUAGAUGAUGUACU

Forward: Score: 151.000000 Q:2 to 18 R:2 to 20 Align Len (16) (75.00%) (81.25%)

Query: 3' ucaUGUAGUAGAUAUGACAu 5'

| ||:|| |||||||

Ref: 5' tacAAATTAT-AATACTGTg 3'

Energy: -12.010000 kCal/Mol

Scores for this hit:
>hsa-miR-144-3p: hsa_circ_0093509: 151.00 -12.01 2 18 2 20 16 75.00% 81.25%

The binding site is located relatively upstream. Since the target gene is a circular RNA, a sequence was taken from the end and appended to the front to design the wild-type and mutant constructs.

>hsa_circ_0093509 WT-hsa-miR-144-3p:
AGAGCACTTAAGAATTCACAGTGTTACAAATTATAATACTGTGGTAGAAACAAATTCAGA
TTCAGATGAT
>hsa_circ_0093509 MUT-hsa-miR-144-3p:
AGAGCACTTAAGAATTCACAGTGTTACTATAATAATATGACAGGTAGAAACAAATTCAGA
TTCAGATGAT